MANCHESTER 1824
The University of Manchester

Ultraviolet radiation drives mutations in a subset of mucosal melanomas

DOI:
10.1038/s41467-020-20432-5

Document Version
Accepted author manuscript

Link to publication record in Manchester Research Explorer

Citation for published version (APA):
Mundra, P., Dhomen, N., Rodrigues, M., Mikkelsen, L. H., Cassoux, N., Brooks, K., Valpione, S., Reis-Filho, J. S., Heegaard, S., Stern, M-H., Roman-Roman, S., & Marais, R. (2021). Ultraviolet radiation drives mutations in a subset of mucosal melanomas. *Nature Communications*, *12*(259), [259]. https://doi.org/10.1038/s41467-020-20432-5

Published in:
Nature Communications

Citing this paper
Please note that where the full-text provided on Manchester Research Explorer is the Author Accepted Manuscript or Proof version this may differ from the final Published version. If citing, it is advised that you check and use the publisher's definitive version.

General rights
Copyright and moral rights for the publications made accessible in the Research Explorer are retained by the authors and/or other copyright owners and it is a condition of accessing publications that users recognise and abide by the legal requirements associated with these rights.

Takedown policy
If you believe that this document breaches copyright please refer to the University of Manchester's Takedown Procedures [http://man.ac.uk/04Y6Bo] or contact uml.scholarlycommunications@manchester.ac.uk providing relevant details, so we can investigate your claim.

Download date:09. Jun. 2022

1 ***Ultraviolet radiation drives mutations in a subset of mucosal melanomas***
2

3 Piyushkumar A. Mundra[1†], Nathalie Dhomen[1†], Manuel Rodrigues[2,3], Lauge Hjorth
4 Mikkelsen[4], Nathalie Cassoux[5], Kelly Brooks[1,6], Sara Valpione[1,7], Jorge S. Reis-
5 Filho[8], Steffen Heegaard[4], Marc-Henri Stern[2,9], Sergio Roman-Roman[10], and Richard
6 Marais[1,*]

7

8 *[1]Molecular Oncology Group, Cancer Research UK Manchester Institute, The*
9 *University of Manchester, Alderley Park, SK10 4TG, UK*
10 *[2]Institut Curie, PSL Research University, INSERM U830, DNA Repair and Uveal*
11 *Melanoma (D.R.U.M.), Equipe labellisée par la Ligue Nationale contre le Cancer,*
12 *Paris 75248, France.*
13 *[3]Institut Curie, PSL Research University, Department of Medical Oncology, Paris*
14 *75248, France.*
15 *[4]Department of Pathology/Eye Pathology Section, University of Copenhagen,*
16 *Rigshospitalet, 2100 Copenhagen, Denmark*
17 *[5]Institut Curie, PSL Research University, Department of Ocular Oncology, Paris*
18 *75248, France.*
19 *[6]QIMR Berghofer Medical Research Institute, Brisbane, Queensland, 4006, Australia*
20 *[7]The Christie NHS Foundation Trust, Manchester, M20 4GJ, UK*
21 *[8]Experimental Pathology Service, Department of Pathology, Memorial Sloan*
22 *Kettering Cancer Center, USA*
23 *[9]Institut Curie, PSL Research University, Department of Genetics, Paris 75248,*
24 *France*
25 *[10]Institut Curie, PSL Research University, Translational Research Department, Paris*
26 *75248, France*
27

28 **Running Title:** UVR exposure is a dominant mutational process in mucosal
29 melanoma

30 **Keywords: UVR, mucosal melanoma, conjunctival melanoma, mutational**
31 **signature**

32 [†]These authors contributed equally to this work.

33 [*]**Correspondence:**
34 Richard Marais, PhD
35 Cancer Research UK Manchester Institute
36 The University of Manchester
37 Alderley Park
38 SK10 4TG, UK
39 Email: richard.marais@cruk.manchester.ac.uk

40 **ABSTRACT**

41 **Although identified as the key environmental driver of common**
42 **cutaneous melanoma, the role of ultraviolet radiation (UVR)-induced DNA**
43 **damage in mucosal melanoma is poorly defined. We analyze 10 mucosal**
44 **melanomas of conjunctival origin by whole genome sequencing and our data**
45 **shows a predominance of UVR-associated single base substitution signature 7**
46 **(SBS7) in the majority of the samples. Our data shows mucosal melanomas with**
47 **SBS7 dominance have similar genomic patterns to cutaneous melanomas and**
48 **therefore this subset should not be excluded from treatments currently used for**
49 **common cutaneous melanoma.**

50

51 **INTRODUCTION**

52 Melanomas are a heterogeneous group of tumors with distinct genomic
53 features that may be broadly classed as epithelium-associated melanomas (includes
54 cutaneous, acral and mucosal melanomas) or non-epithelium associated melanomas
55 (includes uveal and leptomeningeal melanoma)[1]**.** Non-epithelium associated
56 melanomas have distinct clinical and genomic features[1,2], but even among epithelium-
57 associated melanomas, the relative frequency and combinations of genomic
58 alterations vary between subtypes. For example, *KIT* and *SF3B1* mutations are more
59 common in mucosal melanomas, whereas *BRAF* and *NRAS* mutations are more
60 common in common cutaneous melanomas[1].

61 Ultraviolet radiation (UVR)-induced DNA damage is a clinically-relevant
62 factor that distinguishes the different melanoma subtypes[3]. It is clearly linked to the
63 development of common cutaneous melanomas, but its contribution to the rarer
64 subtypes is largely assumed to be negligible, because they tend to arise in sun-

65 protected tissues. Mucosal melanoma (1.4% of melanomas) is an example of such a
66 rare melanoma subtype, which arises in the mucosa of the eyes, mouth, nose, and
67 gastrointestinal and genitourinary tracts. It presents distinct biological and clinical
68 features, responds poorly to treatment, and is characterized by distinct genomic traits,
69 with high numbers of chromosomal structural changes, low mutation burden and
70 specific patterns of driver oncogenes[4,5,6,7,8]. This is thought to be because mucosal
71 melanomas arise in distinct microenvironments and are not driven by UVR[1].
72 However, two recent studies[7,9] reported that 9% (6/67, 6/65 respectively) of mucosal
73 melanomas present >50% of COSMIC single base substitution signature 7 (SBS7), a
74 mutation signature associated with UVR[10]. It was also recently reported that uveal
75 melanoma, another rare melanoma subtype not generally associated with UVR-
76 exposure, can present SBS7-predominance if it arises on the iris[11]. We hypothesized
77 that UVR drives melanomagenesis independent of tissue microenvironment, so to test
78 this we performed whole-genome sequencing (WGS) on mucosal melanomas from
79 the conjunctiva, because this tissue is largely exposed to UVR[12].

80 In this study, we present a comparison of the genomic landscape of these UVR
81 exposed mucosal melanomas to other primary mucosal melanomas and to primary
82 cutaneous melanomas, to provide better understanding of the oncogenes and
83 mutational processes that drive this particular melanoma subtype.

84

85 **RESULTS**

86 **UVR-driven DNA damage is predominant in mucosal melanomas of conjunctival**
87 **origin**

88 We performed (WGS) on 10 fresh frozen primary conjunctival melanomas
89 (median patient age 66 years, range 38-84; 6 females, 4 males; Supplementary Table

1) and compared our results to published WGS from 8 mucosal melanomas originating on sun-protected sites (nasal, genitourinary, rectal; median patient age 63 years, range 46-84; 6 females, 2 males; Supplementary Table 2)[6]. Mutational signature analysis on our WGS data revealed a predominance of COSMIC SBS7v2 in 9 of the conjunctival melanomas, whereas 1 conjunctival melanoma and the other 8 mucosal melanomas were dominated by the SBS1v2 (age-related), SBS5v2 (ubiquitous) and SBS3v2 (*BRCA1, BRCA2* and *PALB2*-associated)(Fig. 1a,b). To facilitate direct comparison with common cutaneous melanoma, we used our pipeline to analyze published WGS from 54 primary common cutaneous melanomas[6] and observed SBS7v2 predominance in 51 of these samples (Fig. 1a,b). Compared to their non-SBS7v2 counterparts, the SBS7v2 mucosal melanomas presented higher proportions of C-to-T transitions at dipyrimidines (mean 84.7 versus 29.0%; P<0.0001; Fig. 1c,d) and higher numbers of single nucleotide variants (SNV)(median 100,098 [range 42,649-274,061] vs. 10,391 [range 8,426-20,538]; P<0.0001; Fig. 1e,f). Similarly, compared to their counterparts, the SBS7v2 cutaneous melanomas presented higher proportions of C-to-T transitions at dipyrimidines (median 82.34% versus 36.09%; P<0.0001; Fig. 1c,d) and higher numbers of SNV (median 119,058 [range 20,021-938,462] vs. 11716 [range 9,838-12,607]; P<0.0001; Fig. 1e,f). Notably, the SBS7v2 mucosal and common cutaneous melanomas presented similar proportions of SNV and C-to-T transitions at dipyrimidines (Fig. 1b,d,f). Equally, the non-SBS7v2 mucosal and common cutaneous melanomas presented similar proportions of SNV, and similar proportions of C-to-T transitions at dipyrimidines (Fig. 1b,d,f) and other nucleotide transitions/transversions (Supplementary Fig. 1a-e). Thus, nine conjunctival mucosal melanomas exhibited features of UVR exposure,

114 whereas one conjunctival and the other 8 mucosal melanomas did not present these
115 features.
116 We validated our findings in an independent cohort of 65 published mucosal
117 melanoma whole genomes[9]. Here we identified 8 samples (12%) with SBS7v2
118 predominance (Supplementary Fig. 2a), which also presented higher SNV loads
119 (Supplementary Fig. 2b), higher proportions of C-to-T transitions at dipyrimidines
120 and lower proportions of other transitions/transversions than their non-SBS7v2
121 counterparts (Supplementary Fig. 2c-h).
122

123 **Structural variants distinguish mucosal melanomas from cutaneous melanomas**
124 **and are independent of UVR mutation signature status**

125 Previous studies have reported increased numbers of structural variants and
126 indels in mucosal melanomas compared to common cutaneous melanomas[6]. We
127 investigated whether UVR-induced DNA damage influenced the extent or pattern of
128 structural variation in mucosal melanomas. Consistent with previous studies[6,7], the
129 mucosal melanomas presented more structural variants and indels than common
130 cutaneous melanomas (Fig 2a). Critically, we observed no significant differences
131 between the SBS7v2-dominant and the non-SBS7v2 cohorts (Fig 2a, Supplementary
132 Fig 3a), and similarly no significant differences in copy number variations (Fig 2b).
133 This was recapitulated in the validation cohort, where we again observed no
134 significant difference in chromosomal structural variants or number of indels between
135 the SBS7v2-dominant and non-SBS7v2 mucosal melanomas (Supplementary Fig.
136 3b,c).
137

138 **SBS7 dominance in mucosal melanoma is a better indicator of UVR-exposure**

139 **than tumor site**

140 Large areas of the conjunctiva are highly sun-exposed, and this is reflected in
141 the SBS7v2 dominance in 9 of 10 genomes from our primary conjunctival
142 melanomas. MuM12, MuM13, MuM16 and MuM17 were localized to the limbus and
143 MuM14 to the upper part of the bulbar conjunctiva, areas that are frequently sun-
144 exposed (Supplementary Table 1). Note however that SBS7v2 also dominated the
145 genomes of MuM10, MuM11 and MuM18, which were from the tarsal conjunctiva
146 which is considered to be more sun-protected, and SBS7v2 dominated the genome of
147 MuM15, which was a large lesion spanning the sun-protected fornix and the sun-
148 exposed caruncle (Supplementary Table 1). Note also that MuM1, which presented
149 the lowest mutation burden and was the only primary conjunctival melanoma that did
150 not exhibit SBS7v2 dominance, arose from the fornix, considered to be the most sun-
151 protected part of the conjunctiva. Similarly, the conjunctival melanoma with the next
152 lowest mutation burden and SBS7v2 contribution was MuM10, another forniceal
153 tumor.

154 In our validation cohort the SBS7v2-dominant mucosal melanomas were from
155 potentially sun-exposed sites, including the lips (3/5), gingiva (2/28), nasal cavity
156 (1/2), multi-sites (lip and gingiva) (1/2) and oropharynx (1/1)[9]. Thus, in these samples
157 also, SBS7v2-dominant mucosal melanomas were largely from potentially sun-
158 exposed sites, but it should be noted that the SBS7v2-domimant mucosal melanomas
159 were still in the minority. Thus, although the precise location of these melanomas is
160 not known, our analysis suggests that the SBS7v2 dominance is a more specific
161 marker of UVR-driven processes than tumor site and henceforth we refer to these
162 tumors as UVR-exposed mucosal melanomas.

163

164 **UVR-exposed mucosal and cutaneous melanomas present similar driver**
165 **oncogene mutations**

166 We next investigated mutations in common melanoma-associated oncogenes.
167 *BRAF* mutations are generally associated with common cutaneous melanoma, but
168 only weakly associated with mucosal melanoma[1]. We observed that 6 of the 9 UVR
169 mucosal melanomas carried *BRAF* mutations, whereas only 1 of the 9 non-UVR
170 mucosal melanomas had a *BRAF* mutation (Fig. 2C). Notably, 8 of the 9 UVR-
171 exposed mucosal melanomas and all 51 UVR-exposed cutaneous melanomas carried
172 mutations in one to eleven known melanoma genes, with the remaining mucosal
173 melanoma (MuM10) carrying a frame-shift mutation in the melanocyte gene *TYRP1*
174 (Fig. 2c; Supplementary Data 1). Thus, *FGFR2/4, ERBB4*, *NF1*, *CDKN2A*, *NFKBIE*,
175 *SALL4*, *TERT*, *GRIN2A* and *TP53* mutations were restricted to UVR-exposed
176 melanomas (Fig. 2c). Conversely, the non-UVR-exposed mucosal and cutaneous
177 melanomas carried mutations in only two (1 sample), one (5 samples) or none (6
178 samples) of the melanoma genes (Fig 2c). Additionally, 31 (52%) UVR-exposed
179 melanomas had *TERT* and/or *TERT* promoter mutations, but only 1 (8%) non-UVR-
180 exposed melanoma had a mutation in this gene (Fig. 2c,d). These data show
181 remarkable enrichment for the same driver oncogene mutations in UVR-exposed
182 cutaneous melanoma and UVR-exposed mucosal melanoma.

183

184 **10-gene panel as surrogate to UVR signature in mucosal melanomas**

185 We previously reported that mutations in a 10-gene panel (*LRP1B, GPR98,*
186 *XIRP2, PKHD1L1, USH2A, DNAH9, PCDH15, DNAH10, TP53, PCDHAC1*) were a
187 surrogate of UVR exposure[3]. We therefore investigated if this panel could segregate
188 UVR-exposed from non-UVR exposed mucosal melanomas. Remarkably, this panel

189 correctly segregated 71/72 (97%) of the UVR-exposed mucosal and cutaneous
190 melanomas (Fig. 2e), including all 9 UVR mucosal melanomas, 8 of which carried
191 mutations in two or more of these genes (Fig. 2e). This panel therefore provides a
192 targeted approach that allows rapid screening for UVR-exposed mucosal melanomas.

193 **DISCUSSION**

194 Although our cohort was small due to the challenges inherent in obtaining
195 samples, we present WGS for 10 conjunctival melanomas, and our results extend
196 previous studies by showing that conjunctival mucosal melanomas have similar
197 genomes to common cutaneous melanoma[12,13,14]. We also show that like common
198 cutaneous melanoma[3], mucosal melanomas present two broad groups, one with
199 SBS7v2 predominance that appears to be UVR-driven, and one that is not UVR-
200 driven, but curiously, both groups present the large structural alterations more
201 commonly observed in mucosal melanoma. Our analysis revealed particularly striking
202 similarities between UVR-exposed mucosal melanomas and UVR-driven common
203 cutaneous melanomas, as both presented high mutation burdens and abundant
204 mutations that activate the BRAF-ERK pathway.

205 Notably, *BRAF* mutations are rare in mucosal melanoma compared to
206 common cutaneous melanoma[15,16], so *BRAF* mutation testing is not recommended or
207 reimbursed in some jurisdictions. However, we show that UVR-driven mucosal
208 melanomas harbor high frequency *BRAF* mutations, so could benefit from BRAF and
209 MEK targeted therapies. We note that the first published case of a patient with a
210 *BRAF*-mutated metastatic conjunctival melanoma treated with vemurafenib was
211 published seven years after the first clinical results of this drug[17], five years after FDA
212 approval for cutaneous melanoma patients[18]. Moreover, although *CKIT* mutations are
213 present in about 15% of mucosal melanomas[1] response rates to KIT inhibitors range

214 from only 5 to 26%, and no KIT drugs are approved for use in these patients.

215 Mucosal melanoma patients are unfortunately also generally excluded from 216 immunotherapy trials[19-21] and because of this exclusion, immunotherapies are not 217 approved for mucosal melanoma in the adjuvant setting. Note however that response 218 rates to immune checkpoint inhibitors in advanced mucosal melanomas are at least 219 half of that seen in non-glabrous skin melanomas[22,23], and it was recently reported that 220 four of five conjunctival melanoma patients responded to immunotherapy[24]. The clear 221 similarities between UVR-driven cutaneous melanoma and UVR-associated mucosal 222 melanoma suggests that mucosal melanoma patients with SBS7v2 predominance may 223 benefit from BRAF/MEK inhibitor combinations and from immunotherapies in both 224 the advanced and adjuvant settings.

225 Despite the similarities in mutation burden and oncogene pathway activation, 226 we note that chromosomal structural variations did not distinguish UVR from non-227 UVR mucosal melanomas, but did distinguish mucosal from common cutaneous 228 melanoma. This suggests that UVR imposes additional processes over the 229 microenvironment-specific mutational processes that otherwise drive the different 230 melanoma subtypes. Together, these data show us that mucosal melanomas do not 231 belong to a homogeneous group of diseases and suggest that tumors arising from 232 mucosal melanocytes are subject to a common tumorigenic process resulting in the 233 accumulation of structural genome variations, to which are added UVR-driven 234 processes in a subset of cases. This aligns with recent reports that *SF3B1* R625 235 mutations are recurrently present in vulvo-vaginal and anorectal melanomas but not in 236 other mucosal locations[25,26]. Our study therefore contributes to the definition of 237 biologically and clinically relevant subsets of mucosal melanomas, providing better 238 insight into their biology and opening avenues for precision medicine.

239 The UVR-driven mucosal melanomas tend to arise on sun-exposed sites such
240 as the conjunctiva and lips, but sun exposure *per se* does not identify this subset of
241 mucosal melanomas, as highlighted by the presence of non-SBS7v2 tumors at
242 potentially sun-exposed sites and SBS7v2 tumors at more sun-protected sites. Some
243 of our SBS7v2 cases came from gingiva, oropharynx or nasal cavity. Whilst
244 imprecision in site reporting may play a role in this, one possibility is that mucosal
245 cells in sun-exposed sites may accumulate UVR-induced mutations and expand into
246 large clones of mutant cells, extending into sun-protected areas where such cells could
247 further develop into a melanoma. Clonal expansions of this nature have been reported
248 in the skin [27] and in Barrett's esophagus[28]. Conversely, the presence of non-SBS7v2
249 tumors at potentially sun-exposed sites is consistent with our previously report that in
250 a UVR/BRAF^{V600E}-driven mouse melanoma model, a small number of tumors
251 developed without evidence of UVR-associated DNA damage[3]. As outlined above,
252 distinguishing UVR and non-UVR melanomas in the mucosal and other settings could
253 have important implications for clinical care. Our data shows that this cannot be
254 determined by the site of the primary tumor, but we propose that our 10-gene panel
255 could provide rapid testing for the UVR signature without the cost and complexity of
256 WGS. Together with the knowledge that the UVR-associated mucosal melanomas
257 could benefit from treatments currently used in common cutaneous melanoma, our
258 findings highlight an approach to delivering precision medicine to this patient group
259 for whom current treatment options are limited.

260

261 METHODS

262 Sample Collection and Ethics

263 Conjunctival melanoma samples MuM1 and MuM10-18 comprise two cohorts, one
264 from Institut Curie, Paris (MuM10, MuM12, MuM15-18) and one from the
265 department of Pathology/Eye Pathology Section, University of Copenhagen,
266 Rigshospitalet (MuM1, MuM11, MuM13, MuM14). The studies were approved by
267 the Internal Review Board of Institut Curie (2014) and the Danish National Ethics
268 Committee (j.no. 1700673) respectively. The samples were collected during surgery
269 and frozen immediately. Paired blood samples were also collected and stored for
270 sequencing. Patients provided written informed consent to perform germline and
271 somatic genetic analyses for whole-genome sequencing on archived frozen samples.
272

273 **DNA extraction and whole genome sequencing**

274 For Institut Curie cohort, DNA was extracted by the *Centre de Ressources*
275 *Biologiques* (Institut Curie tumor biobank) from frozen samples using phenol
276 (Invitrogen) then subsequently purified on Zymo-Spin IC (Zymo Research). DNA
277 was extracted from paired whole blood samples using the QuickGene DNA whole-
278 blood kit with QuickGene-610L equipment (Fujifilm, Japan). DNA concentrations
279 were quantified by Qubit (Thermo Fisher Scientific). Integrities were assessed by a
280 BioAnalyzer 2100 device (Agilent Technologies, Santa Clara, CA, USA). For
281 Rigshospitalet cohort, DNA/RNA was extracted from frozen tumor samples using
282 Norgen (Biotek Corp.) kit and from blood samples using QIAamp DNA Blood and
283 Tissue kit (Qiagen, Manchester, UK) as per manufacturer's instructions.
284 Concentrations were quantified by Qubit (Thermo Fisher Scientific).
285

286 **Sequencing and processing**

287 Whole genome sequencing (WGS) of the tumor-normal pairs from patients included
288 in the Institut Curie cohort (MuM10, MuM12, MuM15-18) was performed in the New
289 York Genome Center (NYGC). DNA libraries were prepared using TruSeq PCR-free
290 approach following the protocols implemented in the NYGC. WGS of the tumor-
291 normal pairs of the Rigshospitalet cohort (MuM1, MuM11, MuM13, MuM14) was
292 performed by Edinburgh Genomics (The Roslin Institute, University of Edinburgh)
293 using TruSeq Nano library preparation method. Sequencing was performed on
294 Illumina HiSeqX machine for both the cohorts with aimed coverage of 30X and 60X
295 for normal (blood) and tumor samples respectively.
296 Whole genome sequencing BAM files of other primary mucosal melanomas (MuM2-
297 MuM9) and primary cutaneous melanomas[6] (Cut1-Cut54) were downloaded from
298 EGA using accession ID EGAS00001001552 using ASPERA(v3.5.4).
299
300 **Bioinformatics Analysis**
301 FASTQ files were extracted for BAM files for MuM2-MuM9 and cutaneous
302 melanoma samples using samtools[29] (v1.3.1). The 2 x 150 read pairs were mapped to
303 the reference genome GRCh37 (v75) using BWA-mem[30] (v0.7.7) tool. This was
304 followed by duplicate removal using PICARD (v1.96) and INDELs realignment and
305 recalibration of base qualities using GATK[31] (v3.6).
306
307 The final BAM files from both tumor and corresponding blood sample were used for
308 subsequent somatic variant calling using MUTECT[32] (v1.1.7) with default
309 parameters. Small insertions and deletions were determined using Strelka[33] (v1.0.4).
310 Only “Passed” calls were considered. Variant effect predictor[34] (Ensembl version 73)
311 was used to annotate the mutations. Known variants present in dbSNP were excluded.

312 Structural variants were determined using DELLY[35] (v0.8.1) with default parameters.

313

314 Mutational signatures were determined by fitting somatic single nucleotide variants
315 with tri-nucleotide context to the 30 COSMIC mutational signatures using
316 deconstructSigs(v1.8.0)[36] package using default parameters. Signatures with
317 contribution weights less than 6% were excluded.

318

319 Copy number alterations were determined using Sequenza[37] (v2.1.9999b0) package
320 with parameters (mufreq.treshold = 0.05, min.reads = 10, min.fw.freq = -0.1). One
321 cutaneous sample with missing gender information in clinical data was excluded from
322 the analysis. Fraction of genomic alteration for each sample was calculated using an
323 in-house script.

324

325

326 **DATA AVAILABILITY**

327 The whole-genome sequencing data generated in this study from conjunctival
328 melanoma samples have been deposited in the EGA database under accession code
329 EGAS00001004697 [https://www.ebi.ac.uk/ega/studies/EGAS00001004697]. The
330 data is available under restricted access, which can be obtained by contacting Prof
331 Richard Marais. The whole-genome sequencing data corresponding to cutaneous
332 melanoma and other mucosal melanoma samples is available from the EGA database
333 under accession code EGAS00001001552
334 [https://www.ebi.ac.uk/ega/studies/EGAS00001001552].

335 **CODE AVAILABILITY**

336 In-house codes used to compute fraction of genome altered are available at:
337 https://github.com/mpiyush21/MucosalNatureComms.

338

339 **ACKNOWLEDGEMENTS**

340 R.M. is supported by Wellcome Trust (100282/Z/12/Z), European Research Council
341 (ERC-ADG-2014 671262), Cancer Research UK (A27412 and A22902). M.R. and
342 M-H.S. are funded by Institut Curie, the Ligue Nationale Contre le Cancer
343 (Labellisation), and Site de Recherche Intégrée sur le Cancer (SiRIC) de l'Institut
344 Curie. M-H.S. is also funded by Institut National de la Santé et de la Recherche
345 Médicale. L.H.M. was funded by a non-restricted Candys Foundation grant. J.S.R.-F.
346 is funded in part the Breast Cancer Research Foundation. S.V. is supported by a Harry
347 J Lloyd Charitable Trust. WGS costs were partly supported by the Manchester NIHR
348 Biomedical Research Centre.

349

350 AUTHOR CONTRIBUTIONS

351 Conceptualization, P.A.M., M.R., L.H.M., N.D., and R.M; Methodology K.B., S.V.,
352 N.C., J.S.R-F; Formal analysis, P.A.M., M.R., L.H.M., and N.D.; Resources, M.R.,
353 L.H.M., N.C., S.H., M-H.S. and S.R., J.S.R-F; Writing, P.A.M., N.D. and R.M;
354 Supervision, S.H., M-H.S., S.R. and R.M.

355

356 COMPETING INTERESTS

357 R.M. consultants for Pfizer, and as a former Institute of Cancer Research (London)
358 employee, he may benefit from commercialized programs. J.S.R.F. consultants for
359 Goldman Sachs, REPARE Therapeutics and Paige.AI, and serves on the scientific
360 advisory boards of Volition Rx and Paige.AI, and ad hoc on the scientific advisory
361 boards of Ventana Medical Systems, Roche Tissue Diagnostics, Genentech, Novartis
362 and InVicro. All other authors declare no competing interests.

363

364 REFERENCES

365

366 1 Bastian, B. C. The molecular pathology of melanoma: an integrated
367 taxonomy of melanocytic neoplasia. *Annu Rev Pathol* **9**, 239-271,
368 doi:10.1146/annurev-pathol-012513-104658 (2014).
369 2 Robertson, A. G. *et al.* Integrative Analysis Identifies Four Molecular and
370 Clinical Subsets in Uveal Melanoma. *Cancer Cell* **32**, 204-220 e215,
371 doi:10.1016/j.ccell.2017.07.003 (2017).
372 3 Trucco, L. D. *et al.* Ultraviolet radiation-induced DNA damage is
373 prognostic for outcome in melanoma. *Nat Med* **25**, 221-224,
374 doi:10.1038/s41591-018-0265-6 (2019).
375 4 Tyrrell, H. & Payne, M. Combatting mucosal melanoma: recent advances
376 and future perspectives. *Melanoma Manag* **5**, MMT11, doi:10.2217/mmt-
377 2018-0003 (2018).
378 5 Furney, S. J. *et al.* Genome sequencing of mucosal melanomas reveals that
379 they are driven by distinct mechanisms from cutaneous melanoma. *J*
380 *Pathol* **230**, 261-269, doi:10.1002/path.4204 (2013).

6 Hayward, N. K. *et al.* Whole-genome landscapes of major melanoma subtypes. *Nature* **545**, 175-180, doi:10.1038/nature22071 (2017).

7 Newell, F. *et al.* Whole-genome landscape of mucosal melanoma reveals diverse drivers and therapeutic targets. *Nat Commun* **10**, 3163, doi:10.1038/s41467-019-11107-x (2019).

8 Mikkelsen, L. H. *et al.* Mucosal malignant melanoma - a clinical, oncological, pathological and genetic survey. *APMIS* **124**, 475-486, doi:10.1111/apm.12529 (2016).

9 Zhou, R. *et al.* Analysis of Mucosal Melanoma Whole-Genome Landscapes Reveals Clinically Relevant Genomic Aberrations. *Clin Cancer Res* **25**, 3548-3560, doi:10.1158/1078-0432.CCR-18-3442 (2019).

10 Alexandrov, L. B. *et al.* Signatures of mutational processes in human cancer. *Nature* **500**, 415-421, doi:10.1038/nature12477 (2013).

11 Johansson, P. A. *et al.* Whole genome landscapes of uveal melanoma show an ultraviolet radiation signature in iris tumours. *Nat Commun* **11**, 2408, doi:10.1038/s41467-020-16276-8 (2020).

12 Rivolta, C. *et al.* UV light signature in conjunctival melanoma; not only skin should be protected from solar radiation. *J Hum Genet* **61**, 361-362, doi:10.1038/jhg.2015.152 (2016).

13 Griewank, K. G. *et al.* Conjunctival melanomas harbor BRAF and NRAS mutations and copy number changes similar to cutaneous and mucosal melanomas. *Clin Cancer Res* **19**, 3143-3152, doi:10.1158/1078-0432.CCR-13-0163 (2013).

14 Swaminathan, S. S. *et al.* Molecular Characteristics of Conjunctival Melanoma Using Whole-Exome Sequencing. *JAMA Ophthalmol* **135**, 1434-1437, doi:10.1001/jamaophthalmol.2017.4837 (2017).

15 Cosgarea, I. *et al.* Targeted next generation sequencing of mucosal melanomas identifies frequent NF1 and RAS mutations. *Oncotarget* **8**, 40683-40692, doi:10.18632/oncotarget.16542 (2017).

16 Flaherty, K. T., Hodi, F. S. & Bastian, B. C. Mutation-driven drug development in melanoma. *Curr Opin Oncol* **22**, 178-183, doi:10.1097/cco.0b013e32833888ee (2010).

17 Flaherty, K. *et al.* Phase I study of PLX4032: Proof of concept for V600E BRAF mutation as a therapeutic target in human cancer. *Journal of Clinical Oncology* **27**, 9000-9000, doi:10.1200/jco.2009.27.15_suppl.9000 (2009).

18 Maleka, A., Astrom, G., Bystrom, P. & Ullenhag, G. J. A case report of a patient with metastatic ocular melanoma who experienced a response to treatment with the BRAF inhibitor vemurafenib. *BMC Cancer* **16**, 634, doi:10.1186/s12885-016-2657-7 (2016).

19 Weber, J. *et al.* Adjuvant Nivolumab versus Ipilimumab in Resected Stage III or IV Melanoma. *N Engl J Med* **377**, 1824-1835, doi:10.1056/NEJMoa1709030 (2017).

20 Eggermont, A. M. M. *et al.* Adjuvant Pembrolizumab versus Placebo in Resected Stage III Melanoma. *N Engl J Med* **378**, 1789-1801, doi:10.1056/NEJMoa1802357 (2018).

21 Robert, C. *et al.* Pembrolizumab versus Ipilimumab in Advanced Melanoma. *N Engl J Med* **372**, 2521-2532, doi:10.1056/NEJMoa1503093 (2015).

429 22 Mignard, C. *et al.* Efficacy of Immunotherapy in Patients with Metastatic
430 Mucosal or Uveal Melanoma. *J Oncol* **2018**, 1908065,
431 doi:10.1155/2018/1908065 (2018).
432 23 Nathan, P. *et al.* Safety and efficacy of nivolumab in patients with rare
433 melanoma subtypes who progressed on or after ipilimumab treatment: a
434 single-arm, open-label, phase II study (CheckMate 172). *Eur J Cancer* **119**,
435 168-178, doi:10.1016/j.ejca.2019.07.010 (2019).
436 24 Sagiv, O. *et al.* Immunotherapy With Programmed Cell Death 1 Inhibitors
437 for 5 Patients With Conjunctival Melanoma. *JAMA Ophthalmol* **136**, 1236-
438 1241, doi:10.1001/jamaophthalmol.2018.3488 (2018).
439 25 Quek, C. *et al.* Recurrent hotspot SF3B1 mutations at codon 625 in
440 vulvovaginal mucosal melanoma identified in a study of 27 Australian
441 mucosal melanomas. *Oncotarget* **10**, 930-941,
442 doi:10.18632/oncotarget.26584 (2019).
443 26 Yang, H. M. *et al.* Identification of recurrent mutational events in anorectal
444 melanoma. *Mod Pathol* **30**, 286-296, doi:10.1038/modpathol.2016.179
445 (2017).
446 27 Klein, A. M., Brash, D. E., Jones, P. H. & Simons, B. D. Stochastic fate of p53-
447 mutant epidermal progenitor cells is tilted toward proliferation by UV B
448 during preneoplasia. *Proc Natl Acad Sci U S A* **107**, 270-275,
449 doi:10.1073/pnas.0909738107 (2010).
450 28 Maley, C. C. *et al.* Selectively advantageous mutations and hitchhikers in
451 neoplasms: p16 lesions are selected in Barrett's esophagus. *Cancer Res*
452 **64**, 3414-3427, doi:10.1158/0008-5472.CAN-03-3249 (2004).
453 29 Li, H. *et al.* The Sequence Alignment/Map format and SAMtools.
454 *Bioinformatics* **25**, 2078-2079, doi:10.1093/bioinformatics/btp352
455 (2009).
456 30 Li, H. & Durbin, R. Fast and accurate short read alignment with Burrows-
457 Wheeler transform. *Bioinformatics* **25**, 1754-1760,
458 doi:10.1093/bioinformatics/btp324 (2009).
459 31 McKenna, A. *et al.* The Genome Analysis Toolkit: a MapReduce framework
460 for analyzing next-generation DNA sequencing data. *Genome Res* **20**,
461 1297-1303, doi:10.1101/gr.107524.110 (2010).
462 32 Cibulskis, K. *et al.* Sensitive detection of somatic point mutations in
463 impure and heterogeneous cancer samples. *Nat Biotechnol* **31**, 213-219,
464 doi:10.1038/nbt.2514 (2013).
465 33 Kim, S. *et al.* Strelka2: fast and accurate calling of germline and somatic
466 variants. *Nat Methods* **15**, 591-594, doi:10.1038/s41592-018-0051-x
467 (2018).
468 34 McLaren, W. *et al.* The Ensembl Variant Effect Predictor. *Genome Biol* **17**,
469 122, doi:10.1186/s13059-016-0974-4 (2016).
470 35 Rausch, T. *et al.* DELLY: structural variant discovery by integrated paired-
471 end and split-read analysis. *Bioinformatics* **28**, i333-i339,
472 doi:10.1093/bioinformatics/bts378 (2012).
473 36 Rosenthal, R., McGranahan, N., Herrero, J., Taylor, B. S. & Swanton, C.
474 DeconstructSigs: delineating mutational processes in single tumors
475 distinguishes DNA repair deficiencies and patterns of carcinoma
476 evolution. *Genome Biol* **17**, 31, doi:10.1186/s13059-016-0893-4 (2016).

477 37 Favero, F. *et al.* Sequenza: allele-specific copy number and mutation
478 profiles from tumor sequencing data. *Ann Oncol* **26**, 64-70,
479 doi:10.1093/annonc/mdu479 (2015).
480

481

482 **FIGURE LEGENDS**

483 **Figure 1: Mutation spectra in mucosal and common cutaneous melanomas.**

484 **a** Mutation signatures weighted by relative contribution to spectrum of mutations in
485 individual tumor genomes. Indices above indicate mucosal (black, n=18) or common
486 cutaneous (red, n=54) melanomas with subdivision into non-SBS7v2 (blue, n=9, n=3
487 respectively) and SBS7v2 (magenta, n=9, n=51 respectively) genomes. Columns
488 represent individual tumors. **b** Relative contribution of SBS7v2 to mutation spectra
489 (SBS7v2 Weights) for individual mucosal (MuM) or cutaneous (Cut) melanomas with
490 SBS7v2 (magenta n=9, grey n=51) or non-SBSv2 (maroon n=9, blue n=3) genomes. **c**
491 Proportion of six nucleotide transitions/transversions for individual tumor genomes
492 (individual columns). **d** Proportions of C>T nucleotide transitions in individual
493 mucosal (MuM) or cutaneous (Cut) melanomas with SBS7v2-dominant (magenta
494 n=9, grey n=51) or non-SBSv2 (maroon n=9, blue n=3) genomes. **e** Total SNVs in
495 individual mucosal (MuM, magenta, n=18) or cutaneous (Cut, grey, n=54)
496 melanomas. Columns represent individual tumors. **f** Total SNVs in mucosal (MuM)
497 and cutaneous (Cut) melanomas with SBS7v2-predominant (magenta n=9, grey n=54)
498 or non-SBSv2 (maroon n=9, blue n=3) genomes. Panels (b, d, f) show median and
499 95% confidence intervals, dots denote individual tumors, p-values determined by two-
500 tailed Mann Whitney U, ns= not significant: 0.4140 in b, 0.8387 in d, 0.6838 in f,
501 respectively).

502 **Figure 2: Structural alterations and gene mutations in mucosal and common**
503 **cutaneous melanomas.**

504 **a** Numbers and types of structural variants in individual melanoma genomes. Indices
505 above indicate mucosal (black, n=18) and common cutaneous (red, n=54) melanomas

506 with subdivision into non-SBS7v2 (blue; n=9, n=3 respectively) and SBS7v2-
507 dominant (magenta; n=9, n=51 respectively) genomes. Columns represent individual
508 tumors. **b** Relative amounts of chromosomal gains and losses (fraction of genome) in
509 individual genomes. Columns represent individual tumors. **c,d** Missense (orange) or
510 frameshift (blue) mutations in known melanoma oncogenes (**c**), or *TERT* promoter
511 regions (**d**) of individual tumors. **e** Missense mutations (orange) in the indicated genes
512 for individual tumors (columns). Dotted lines denote segregation into non-SBS7v2
513 and SBS7v2 dominant genomes.

514

515

Figure 1

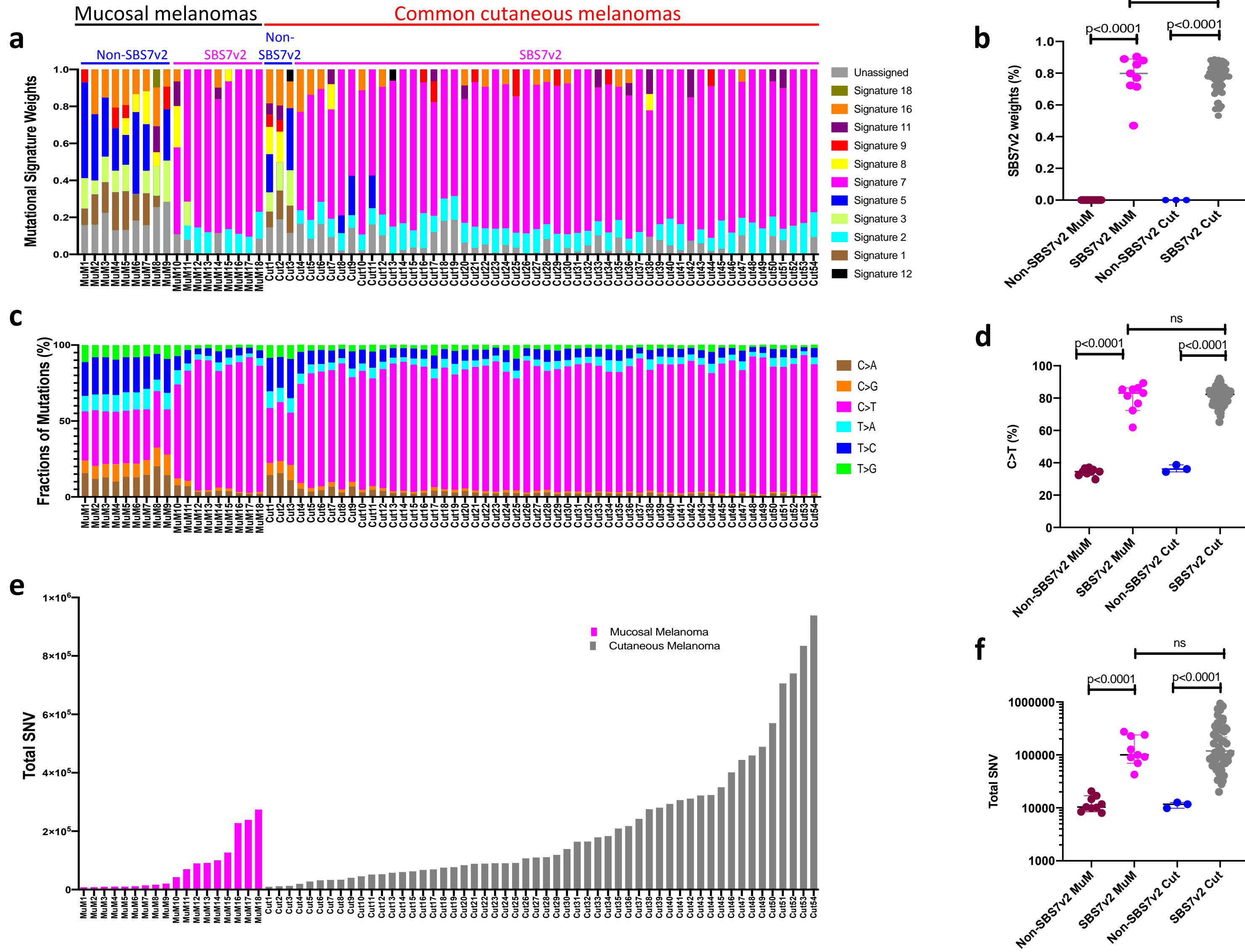

Figure 2

Mucosal melanomas
Common cutaneous melanomas

a

Non-SBS7v2
SBS7v2
Non-SBS7v2
SBS7v2

Numbers of Structural Variants
0
100
200
300
400

Duplication
Deletion
Inversion
Translocation

MuM1 MuM2 MuM3 MuM4 MuM5 MuM6 MuM7 MuM8 MuM9 MuM10 MuM11 MuM12 MuM13 MuM14 MuM15 MuM16 MuM17 MuM18 Cut1 Cut2 Cut3 Cut4 Cut5 Cut6 Cut7 Cut8 Cut9 Cut10 Cut11 Cut12 Cut13 Cut14 Cut15 Cut16 Cut17 Cut18 Cut19 Cut20 Cut21 Cut22 Cut23 Cut24 Cut25 Cut26 Cut27 Cut28 Cut29 Cut30 Cut31 Cut32 Cut33 Cut34 Cut35 Cut36 Cut37 Cut38 Cut39 Cut40 Cut41 Cut42 Cut43 Cut44 Cut45 Cut46 Cut47 Cut48 Cut49 Cut50 Cut51 Cut52 Cut53 Cut54

b

Fraction of Genome
0.0
0.5
1.0

Gain
Loss

MuM1 MuM2 MuM3 MuM4 MuM5 MuM6 MuM7 MuM8 MuM9 MuM10 MuM11 MuM12 MuM13 MuM14 MuM15 MuM16 MuM17 MuM18 Cut1 Cut2 Cut3 Cut4 Cut5 Cut6 Cut7 Cut8 Cut9 Cut10 Cut11 Cut12 Cut13 Cut14 Cut15 Cut16 Cut17 Cut18 Cut19 Cut20 Cut21 Cut22 Cut23 Cut24 Cut25 Cut26 Cut27 Cut28 Cut29 Cut30 Cut31 Cut32 Cut33 Cut34 Cut35 Cut36 Cut37 Cut38 Cut39 Cut40 Cut41 Cut42 Cut43 Cut44 Cut45 Cut46 Cut47 Cut48 Cut49 Cut50 Cut51 Cut52 Cut53 Cut54

c

BRAF
NRAS
NF1
KIT
CDKN2A
FGFR2
FGFR4
MAP3K1
ERBB4
NFKBIE
SALL4
TERT
GRIN2A
TP53
TYRP1

MuM1 MuM2 MuM3 MuM4 MuM5 MuM6 MuM7 MuM8 MuM9 MuM10 MuM11 MuM12 MuM13 MuM14 MuM15 MuM16 MuM17 MuM18 Cut1 Cut2 Cut3 Cut4 Cut5 Cut6 Cut7 Cut8 Cut9 Cut10 Cut11 Cut12 Cut13 Cut14 Cut15 Cut16 Cut17 Cut18 Cut19 Cut20 Cut21 Cut22 Cut23 Cut24 Cut25 Cut26 Cut27 Cut28 Cut29 Cut30 Cut31 Cut32 Cut33 Cut34 Cut35 Cut36 Cut37 Cut38 Cut39 Cut40 Cut41 Cut42 Cut43 Cut44 Cut45 Cut46 Cut47 Cut48 Cut49 Cut50 Cut51 Cut52 Cut53 Cut54

d

TERT (5:1295228)
TERT (5:1295250)

MuM1 MuM2 MuM3 MuM4 MuM5 MuM6 MuM7 MuM8 MuM9 MuM10 MuM11 MuM12 MuM13 MuM14 MuM15 MuM16 MuM17 MuM18 Cut1 Cut2 Cut3 Cut4 Cut5 Cut6 Cut7 Cut8 Cut9 Cut10 Cut11 Cut12 Cut13 Cut14 Cut15 Cut16 Cut17 Cut18 Cut19 Cut20 Cut21 Cut22 Cut23 Cut24 Cut25 Cut26 Cut27 Cut28 Cut29 Cut30 Cut31 Cut32 Cut33 Cut34 Cut35 Cut36 Cut37 Cut38 Cut39 Cut40 Cut41 Cut42 Cut43 Cut44 Cut45 Cut46 Cut47 Cut48 Cut49 Cut50 Cut51 Cut52 Cut53 Cut54

e

DNAH10
DNAH9
GPR98
LRP1B
PCDH15
PCDHAC1
PKHD1L1
USH2A
XIRP2
TP53

MuM1 MuM2 MuM3 MuM4 MuM5 MuM6 MuM7 MuM8 MuM9 MuM10 MuM11 MuM12 MuM13 MuM14 MuM15 MuM16 MuM17 MuM18 Cut1 Cut2 Cut3 Cut4 Cut5 Cut6 Cut7 Cut8 Cut9 Cut10 Cut11 Cut12 Cut13 Cut14 Cut15 Cut16 Cut17 Cut18 Cut19 Cut20 Cut21 Cut22 Cut23 Cut24 Cut25 Cut26 Cut27 Cut28 Cut29 Cut30 Cut31 Cut32 Cut33 Cut34 Cut35 Cut36 Cut37 Cut38 Cut39 Cut40 Cut41 Cut42 Cut43 Cut44 Cut45 Cut46 Cut47 Cut48 Cut49 Cut50 Cut51 Cut52 Cut53 Cut54